In silico discovery of small molecules that inhibit RfaH recruitment to RNA polymerase

Dmitri Svetlov, Da Shi, Joy Twentyman, Yuri Nedialkov, David A. Rosen, Ruben Abagyan and Irina Artsimovitch

SUPPLEMENTARY INFORMATION

Supplementary Table 1: Strains, plasmids and oligonucleotides

Strains		
Name	Features	Reference
MG1655	Wild-type *E. coli*	N. Ruiz
IA228	MG1655 *ΔrfaH*	(Hu & Artsimovitch, 2017)
TOP52	Wild-type *K. pneumoniae*	(Rosen *et al.*, 2018)
TOP52*ΔrfaH*	*rfaH* knockout in TOP52	(Rosen *et al.*, 2018)
Plasmids		
Name	Key features	Reference
pIA947	P_{trc}–no insert; control plasmid; P_{lacIQ1}-*lacI.* P15A origin, Cm^R	(Belogurov *et al.*, 2010)
pIA957	P_{trc}–*E. coli* RfaH; P15A origin, Cm^R	(Belogurov *et al.*, 2010)
pIA1001	P_{trc}–*E. coli* RfaH T66A; P15A origin, Cm^R	(Belogurov *et al.*, 2010)
pIA1003	P_{trc}–*E. coli* RfaH R73D; P15A origin, Cm^R	(Belogurov *et al.*, 2010)
pIA1005	P_{trc}–*E. coli* RfaH R16A*;* P15A origin, Cm^R	(Belogurov *et al.*, 2010)
pIA1006	P_{trc}–*E. coli* RfaH Y54F*;* P15A origin, Cm^R	(Belogurov *et al.*, 2010)
pIA1094	P_{trc}–*E. coli* RfaH I146D; P15A origin, Cm^R	(Burmann *et al.*, 2012)
pIA1282	P_{trc}–*K. pneumoniae* RfaH*;* P15A origin, Cm^R	This work
pHK2	P_{BAD}–*ops*–TC_{15}–*luxCDABE;* pSC101 origin, Sp^R	(Hu & Artsimovitch, 2017)

pIA1283	P_{BAD}–*ops*–*luxCDABE;* pSC101 origin, Sp^R	This work
pIA1297	P_{BAD}–*ops* G8C–*luxCDABE;* pSC101 origin, Sp^R	This work
Oligonucleotides		
Name	Features and sequence	Reference
2536	T7A1 promoter primer; -35, -10 and transcription start site are underlined AAAAAGAGTATTGACTTAAAGTCTAACCTATAGGATACTTACAGCCA TCGAGCAGGCAGCGGCAAAGCCATGG	(Zuber *et al.*, 2018)
2537	Downstream primer: AAATAAGCGGCTCTCAGTTT	(Zuber *et al.*, 2018)
2499	Upstream primer step 2: AAAAAGAGTATTGACTTAAAG	(Zuber *et al.*, 2018)
NT43	Scaffold assembly, nontemplate DNA strand GAAACACCACCAGTAGGCGGTAGCGTGCGTTTTTCGTTCTTCC	(Nedialkov *et al.*, 2018)
T43	Scaffold assembly, template DNA strand GGAAGAACGAAAAACGCACGCTACCGCCTACTGGTGGTGTTTC	(Nedialkov *et al.*, 2018)
R43	Scaffold assembly, RNA strand UUAUUCGGUAGCGU	(Nedialkov *et al.*, 2018)
2141	Upstream Rho terminator primer GTGATAATGGTTGCATGTAGTAAGGAGGTTGTATGGAAGACCGGTA ACATTAATCAACGCGTT	This work
2142	Downstream Rho terminator primer GCGCCTGCAACCGCTGAAATTTG	This work
2143	Upstream λ P_R promoter primer; -35, -10 and start site are underlined CTAACACCGTGCGTGTTGACTATTTTACCTCTGGCGGTGATAATGGTT GCATGTAG	This work

Supplementary Figures

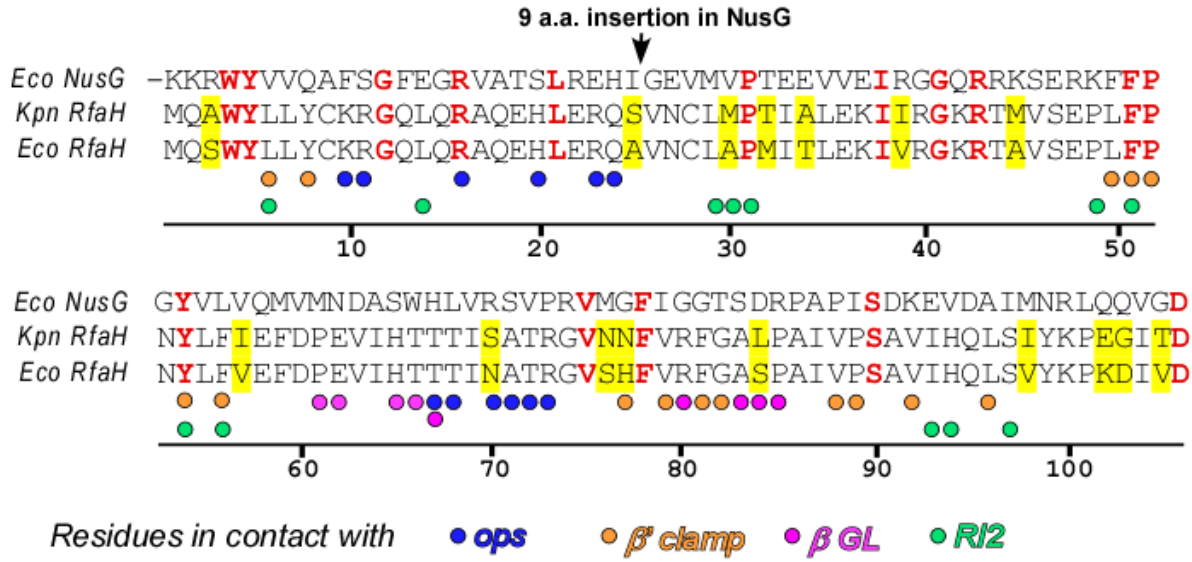

Fig. S1. Structure-based alignment of the Eco RfaH, Eco NusG, and Kpn RfaH NTDs. The numbers below indicate RfaH residues; NusG NTD contains an N-terminal extension and a nine-residue insertion at the indicated position. Residues that are identical in all proteins are shown in red. Residues that differ between Eco and Kpn RfaHs (16 total in the NTD) are highlighted in yellow. Green dots indicate hypothetical contacts between the RfaH-NTD and RI2. Blue, orange, and magenta dots indicate RfaH contacts to the *ops* DNA, the β'CH, and βGL, respectively, observed in the cryoEM structure of RfaH bound to the *E. coli ops* TEC (Kang *et al.*, 2018).

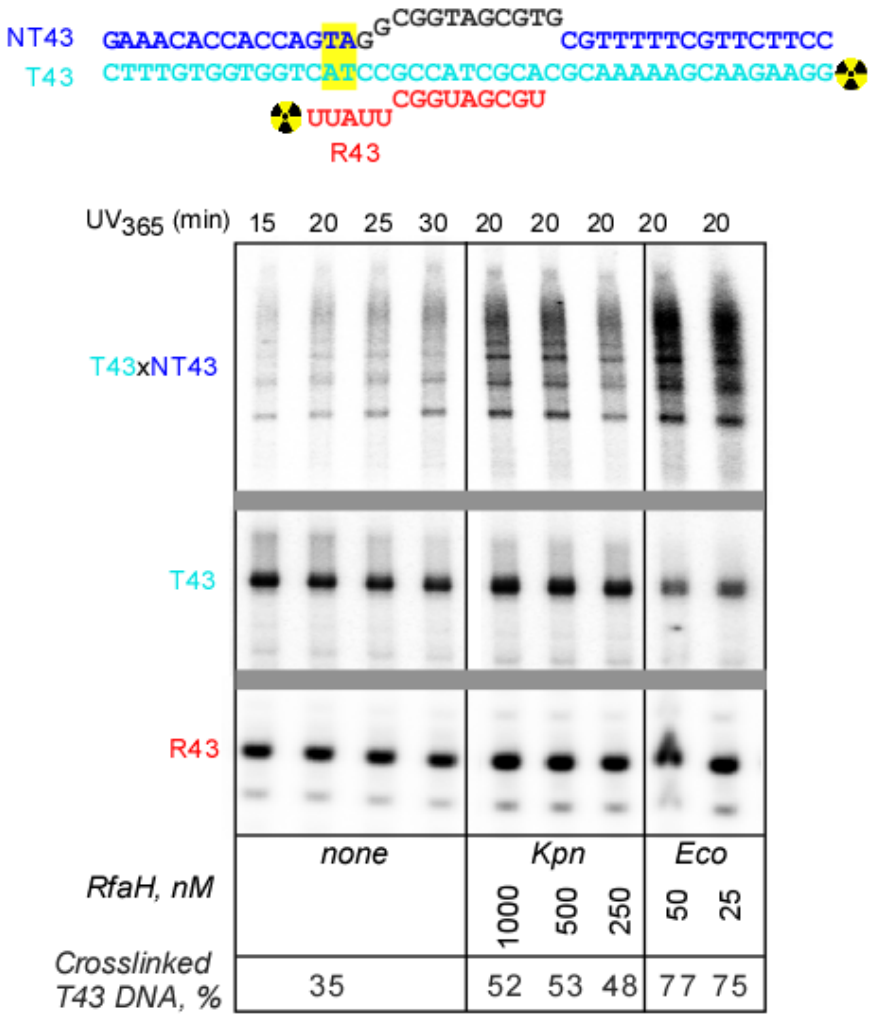

Fig. S2. Assaying the upstream fork junction by psoralen crosslinking. TECs were assembled on the scaffold shown on top, with the template DNA and RNA strands labeled with [γ^{32}P]-ATP. TECs were supplemented with Eco or Kpn RfaH (at indicated concentrations) or storage buffer and illuminated with the 365 nm UV light on ice for 15-30 min (as shown). Samples were mixed with an equal volume of stop buffer and analyzed on a denaturing 12% acrylamide-urea gel. The positions of the RNA, free template DNA (T43) and crosslinked species are indicated. Fractions of the template strand DNA crosslinked after 20 min incubation are indicated below.

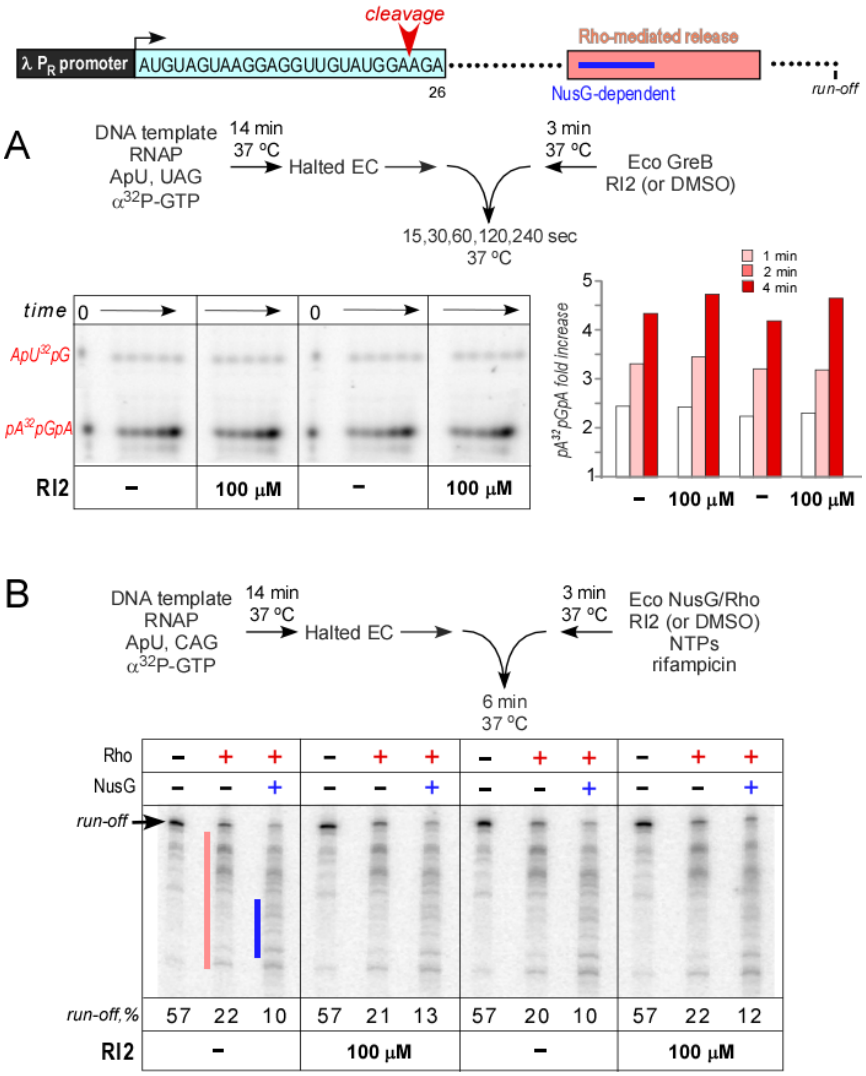

Fig. S3. Analysis of RI effects on Eco GreB, NusG, and Rho transcription factors. A linear PCR-generated DNA template encoding a phage λP_R promoter, an initial 26-nt transcribed region lacking C residues, and a Rho-dependent *yhjG* terminator is shown on top. NusG induces an early RNA release, indicated by a blue bar within the red Rho-dependent release window.

(A) GreB-assisted RNA cleavage assays. Halted α^{32}P-GMP labeled A26 TECs were prepared by withholding CTP. In A26 TECs, the backtracked RNA is susceptible to cleavage, which is greatly enhanced by GreB (Vassylyeva *et al.*, 2007). Eco GreB (200 nM) was preincubated with RI2 (200 μM) or DMSO and mixed with an equal volume of A26 TEC to initiate the reaction; the final concentrations of GreB and RI2 were 100 nM and 100 μM, respectively. Following incubation at 37 °C for the indicated times, the reactions were quenched and analyzed on a 12 % urea-acrylamide (19:1) gel. The $pA^{32}pGpA$ RNA,

generated during repeated cleavage and re-synthesis of A26 RNA, was quantified as a function of time using ApU^{32}pG abortive RNA product as a loading control. Note that ApU^{32}pG migrates slower due to the absence of the 5' phosphate group. A graph on the right shows an increase of pA^{32}pGpA RNA over intrinsic, GreB-independent RNA cleavage (at time 0) as a function of time. Duplicate experiments are shown.

(B) Single-round Rho-dependent termination assays. Eco Rho (40 nM), Eco NusG (300 nM) and RI2 (200 μM) [or DMSO/storage buffers] were preincubated with rifampicin and chase NTPs and mixed with an equal volume of α^{32}P-GMP labeled A26 TECs; the final concentrations of Rho, NusG, and RI2 were 20 nM, 150 nM and 100 μM, respectively. Following a 6-min incubation at 37 ^{o}C, the reactions were quenched and analyzed on a 7 % urea-acrylamide (19:1) gel. Fractions of the full-length run-off RNA determined from duplicate experiments are shown below each panel.

Supplementary references

Belogurov, G.A., A. Sevostyanova, V. Svetlov & I. Artsimovitch, (2010) Functional regions of the N-terminal domain of the antiterminator RfaH. *Mol Microbiol* **76**: 286-301.

Burmann, B.M., S.H. Knauer, A. Sevostyanova, K. Schweimer, R.A. Mooney, R. Landick, I. Artsimovitch & P. Rosch, (2012) An alpha helix to beta barrel domain switch transforms the transcription factor RfaH into a translation factor. *Cell* **150**: 291-303.

Hu, K. & I. Artsimovitch, (2017) A Screen for rfaH Suppressors Reveals a Key Role for a Connector Region of Termination Factor Rho. *MBio* **8**.

Kang, J.Y., R.A. Mooney, Y. Nedialkov, J. Saba, T.V. Mishanina, I. Artsimovitch, R. Landick & S.A. Darst, (2018) Structural Basis for Transcript Elongation Control by NusG Family Universal Regulators. *Cell*.

Nedialkov, Y., D. Svetlov, G.A. Belogurov & I. Artsimovitch, (2018) Locking the non-template DNA to control transcription. *Mol Microbiol*.

Rosen, D.A., J. Twentyman & D.A. Hunstad, (2018) High Levels of Cyclic Di-GMP in Klebsiella pneumoniae Attenuate Virulence in the Lung. *Infect Immun* **86**.

Vassylyeva, M.N., V. Svetlov, A.D. Dearborn, S. Klyuyev, I. Artsimovitch & D.G. Vassylyev, (2007) The carboxy-terminal coiled-coil of the RNA polymerase beta'-subunit is the main binding site for Gre factors. *EMBO Rep* **8**: 1038-1043.

Zuber, P.K., I. Artsimovitch, M. NandyMazumdar, Z. Liu, Y. Nedialkov, K. Schweimer, P. Rosch & S.H. Knauer, (2018) The universally-conserved transcription factor RfaH is recruited to a hairpin structure of the non-template DNA strand. *Elife* **7**.